JOC The Journal of Organic Chemistry

Article

pubs.acs.org/joc

Design, Synthesis, and Properties of Phosphoramidate 2′,5′-Linked Branched RNA: Toward the Rational Design of Inhibitors of the RNA Lariat Debranching Enzyme

Nobuhiro Tago,[†,‡] Adam Katolik,[†] Nathaniel E. Clark,[§] Eric J. Montemayor,[§,⊥] Kohji Seio,[‡] Mitsuo Sekine,[‡] P. John Hart,[§,∥] and Masad J. Damha*[,†]

[†]Department of Chemistry, McGill University, 801 Sherbrooke Street West, Montréal, Québec H3A 0B8, Canada

[‡]Department of Life Science, Tokyo Institute of Technology, 4259 Nagatsuta, Midoriku, Yokohama, Kanagawa 226-8501, Japan

[§]Department of Veterans Affairs, South Texas Veterans Health Care System, San Antonio, Texas 78229, United States

[∥]Department of Biochemistry, University of Texas Health Science Center, 7703 Floyd Curl Drive, San Antonio, Texas 78229, United States

[⊥]Departments of Biochemistry and Biomolecular Chemistry, University of Wisconsin-Madison, 433 Babcock Dr., Madison, Wisconsin 53706, United States

Supporting Information

ABSTRACT: Two RNA fragments linked by means of a 2′,5′ phosphodiester bridge (2′ hydroxyl of one fragment connected to the 5′ hydroxyl of the other) constitute a class of nucleic acids known as 2′-5′ branched RNAs (bRNAs). In this report we show that bRNA analogues containing 2′-5′ phosphoramidate linkages (bN-RNAs) inhibit the lariat debranching enzyme, a 2′,5′-phosphodiesterase that has recently been implicated in neurodegenerative diseases associated with aging. bN-RNAs were efficiently generated using automated solid-phase synthesis and suitably protected branchpoint building blocks. Two orthogonally removable groups, namely the 4-monomethoxytrityl (MMTr) group and the fluorenylmethyl-oxycarbonyl (Fmoc) groups, were evaluated as protecting groups of the 2′ amino functionality. The 2′-*N*-Fmoc methodology was found to successfully produce bN-RNAs on solid-phase oligonucleotide synthesis. The synthesized bN-RNAs resisted hydrolysis by the lariat debranching enzyme (Dbr1) and, in addition, were shown to attenuate the Dbr1-mediated hydrolysis of native bRNA.

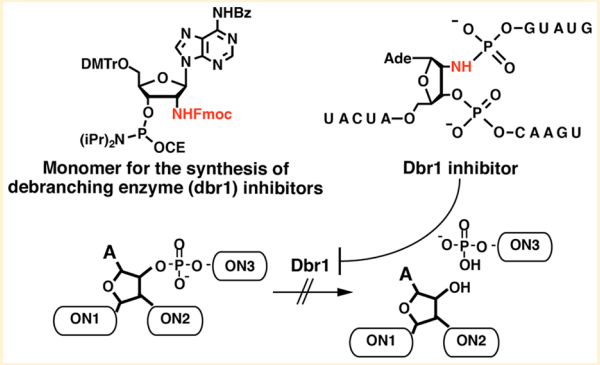

INTRODUCTION

Branched RNAs are important nucleic acid structures generated during messenger RNA (mRNA) maturation in eukaryotic cells. The processing of nascent precursor-mRNA (pre-mRNA) into mature mRNA transcripts involves an editing step known as splicing, during which the noncoding intron sequences are excised and the exon sequences are ligated by the spliceosome in order to generate mature mRNAs.[1−5] The excised introns adopt a "lariat" configuration that contains an atypical 2′,5′-phosphodiester linkage at the branchpoint junction.[6] The hydrolysis of this linkage is mediated by the lariat debranching enzyme (Dbr1) and is necessary for the degradation of lariat introns after they have been excised by the spliceosome.[7] Dbr1 also hydrolyzes the 2′,5′-phosphodiester linkage found in Y-shaped branched RNA (bRNA) and multicopy single stranded DNA (msDNA).[8] In addition, Dbr1 activity is involved in the maturation of small nucleolar RNAs (snoRNA) and micro RNAs (miRNA), whose sequences are encoded within introns.[9−12]

Dbr1 enzymes possess two-domains:[13] an N-terminal domain that belongs to the metallophosphoesterase (MPEs) superfamily of enzymes,[14] and a C-terminal domain that stabilizes the interaction between lariat RNA and a lengthy internal loop unique to Dbr1 MPEs involved in branchpoint recognition.[13] Loss of Dbr1 activity results in accumulation of RNA lariats, which are believed to sequester pathogenic forms of TAR DNA binding protein 43 (TDP-43),[15] an RNA-binding protein implicated in neurodegenerative diseases associated with aging.[16] In spinal cord neurons affected by amyotrophic lateral sclerosis (ALS), inclusions enriched in TDP-43 are hallmarks of the disease. The knockdown of Dbr1 activity in yeast, primary rat neurons, and in a selected human neuronal cell line has been shown to offer protection against TDP-43-mediated toxicity.[17] These observations suggest that the identification of inhibitors of Dbr1 activity could open a

Received: July 24, 2015
Published: September 17, 2015

DOI: 10.1021/acs.joc.5b01719
J. Org. Chem. 2015, 80, 10108−10118

novel therapeutic avenue for the treatment of ALS and the related disorder, frontotemporal lobar degeneration (FTLD).

Structure-guided synthesis of chemically modified RNAs represents a useful strategy for identifying potential Dbr1 inhibitors; and the family of nonhydrolyzable bRNAs that mimic the lariat RNA branchpoints seems most promising. Recently, the crystal structure of purified, recombinant Dbr1 from the amoeba *Entamoeba histolytica* (*Eh*) was determined, providing the first picture of an RNA lariat debranching enzyme in the absence of nucleic acids as well as in complex with several synthetic RNAs.[13] The enzyme engages the branchpoint adenosine nucleotide in a C2′-endo sugar conformation that, together with stacking of the adenine base between His16 and Tyr64, places the pseudo-equatorial 2′ phosphate adjacent to the metal binding center and the 2′-O within hydrogen-bonding distance of His91 (Figure 1). The binding interactions

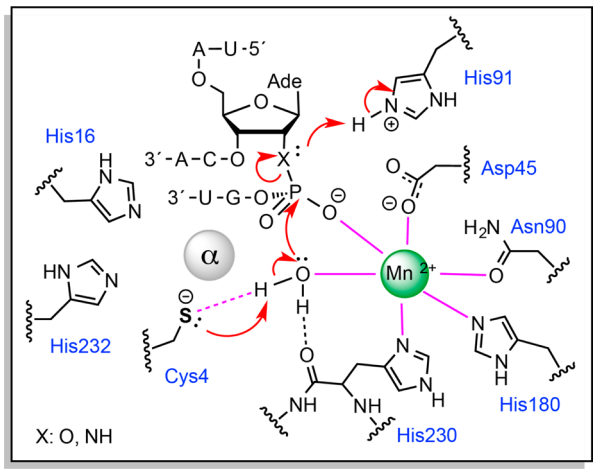

Figure 1. Model of bRNA bound to Dbr1 and proposed hydrolytic mechanism.[13]

between the RNA branchpoint and Dbr1 suggest that the hydrolysis of the 2′,5′-phosphodiester linkage proceeds through a S_N2 inversion mechanism in which the bound metal acts as a Lewis acid, increasing the electrophilic character of the 2′-phosphorus and concomitantly increasing the nucleophilicity of the metal-bound water (Figure 1). The cysteine residue (Cys14) in the active site, invariant in Dbr1 enzymes, might facilitate the attack of the metal-bound water by acting as a catalytic base or by participating in the binding of a second metal ion as is observed in other MPE family members.[14] A putative trigonal bipyramidal transition-state intermediate is resolved by proton transfer to the O2′ leaving group by the putative catalytic acid His91 (Figure 1).

We previously showed that synthetic bRNAs containing a 2′,5′-phosphorothioate (PS) linkage can bind to *Eh*-Dbr1 (C14S mutant), with a 3′,5′-phosphodiester linkage in the active site instead of the expected 2′,5′-linkage.[13] The crystal structure of the 2′,5′-PS-bRNA ·*Eh*Dbr1 complex suggests that the sulfur atom of the phosphorothioate, which has a larger van der Waals radius than that of oxygen ($\Delta r_w \sim 0.3$ Å), sterically hinders the accommodation of the phosphorus linkage within the active site. This prompted us to move toward bRNA analogues containing a phosphoramidate (2′N-PO_2-O5′) bridge instead, as the size of the nitrogen atom more closely resembles that of the natural oxygen atom in the phosphodiester bond. Furthermore, the 2′,5′-phosphoramidate moiety is expected to be more resistant to hydrolysis given that, under neutral or basic conditions, RNH(−) is a poorer leaving group relative to RO(−). Finally, replacing the O2′ by N2′ is expected to steer the sugar pucker toward the C2′-endo pucker,[18] which corresponds to the sugar conformation found in the bRNA·EhDbr1 cocrystal.

Here, we describe the first solid-phase synthesis of bRNAs containing 2′,5′-phosphoramidate moieties ("bN-RNAs"). The synthesized bN-RNAs were evaluated for their biological and chemical stability as well as for their ability to inhibit the activity of Dbr1.

RESULTS AND DISCUSSION

Synthesis of Branched Nucleotides. Our method for unmodified Y-shaped RNA synthesis revolves around the incorporation of a branch-site monomer that allows for the selective growth of each of the three branches regioselectively from any of the hydroxyl positions (5′, 3′, or 2′). This approach generates a TBDMS-protected bRNA that can be deprotected and released from the support under standard conditions.[19,20] In this study, we employed the same strategy to build a phosphoramidate branchpoint, which requires a protecting group at the 2′-amino position that can be removed selectively (orthogonally) during solid-phase synthesis. We considered both the 4-monomethoxytrityl (MMTr)[21] and fluorenylmethyloxycarbonyl (Fmoc)[22,23] groups. They can be removed by an acid and base treatment, respectively, under conditions that do not affect the TBDMS or amide-based *N*-protecting groups commonly used in RNA synthesis.

The MMTr and Fmoc-protected phosphoramidites were prepared following two synthetic routes that are described in Scheme 1. Both routes used N^6-Benzoyl-2′-deoxy-2′-amino-3′,5′-*O*-[1,1,3,3-tetraisopropyl-1,3-disiloxanediyl]adenosine (**1**)[24] as a starting material. The synthesis of the 2′-*N*-MMTr monomer **5** then started with the protection of the amino group by reacting **1** with MMTr-chloride (MMTr-Cl), affording **2** in excellent yield, and was followed by the removal of the 3′,5′-*O*,*O*,-disiloxane bridge using tetra-*n*-butylammonium fluoride (TBAF), yielding **3** in 81%. Next, the 5′ hydroxyl group was esterified with the orthogonally cleavable levulinyl group. Regioselectivity for the 5′ hydroxyl over the 3′ hydroxyl was achieved with a levulinic acid substrate that was preactivated with *O*-(benzotriazol-1-yl)- *N*,*N*,*N*′,*N*′-tetramethyluronium tetrafluoroborate (TBTU) as a coupling reagent. This afforded **4** in 31% yield. Finally, **4** was phosphitylated at the remaining 3′ hydroxyl position under standard conditions, thus generating the first branchpoint synthon **5** in 80% yield. To prepare the alternative, 2′-*N*-Fmoc-protected branching unit **9** (Scheme 1,B), compound **1** was reacted with Fmoc-chloride (FmocCl) in pyridine yielding **6** (89%). Next, the 2′,5′-*O*,*O*-disiloxane bridge was removed using TEA·3HF yielding **7** (75%), followed by the installation of the DMTr group on the 5′ hydroxyl (**8**, 94%). Phosphitylation of the remaining 3′ hydroxyl group of **8** under standard conditions afforded amidite **9** in 80% yield. Before engaging on solid-phase bN-RNA synthesis, the reactivity of the branching amidites under coupling conditions was monitored by ^{31}P NMR spectra to assess the applicability of the amidite for solid-phase bN-RNA synthesis.

Specifically, synthons **5** and **9** were activated with 5-(ethylthio)-1*H*-tetrazole (ETT) or 4,5-dicyanoimidazole (DCI) (general RNA/DNA coupling reagents) in CD_3CN, and ^{31}P NMR spectra were recorded for both compounds

DOI: 10.1021/acs.joc.5b01719
J. Org. Chem. 2015, 80, 10108−10118

Scheme 1. Syntheses of (A) 2′-*N*-MMTr Monomer 5 (B) 2′-*N*-Fmoc Monomer 9

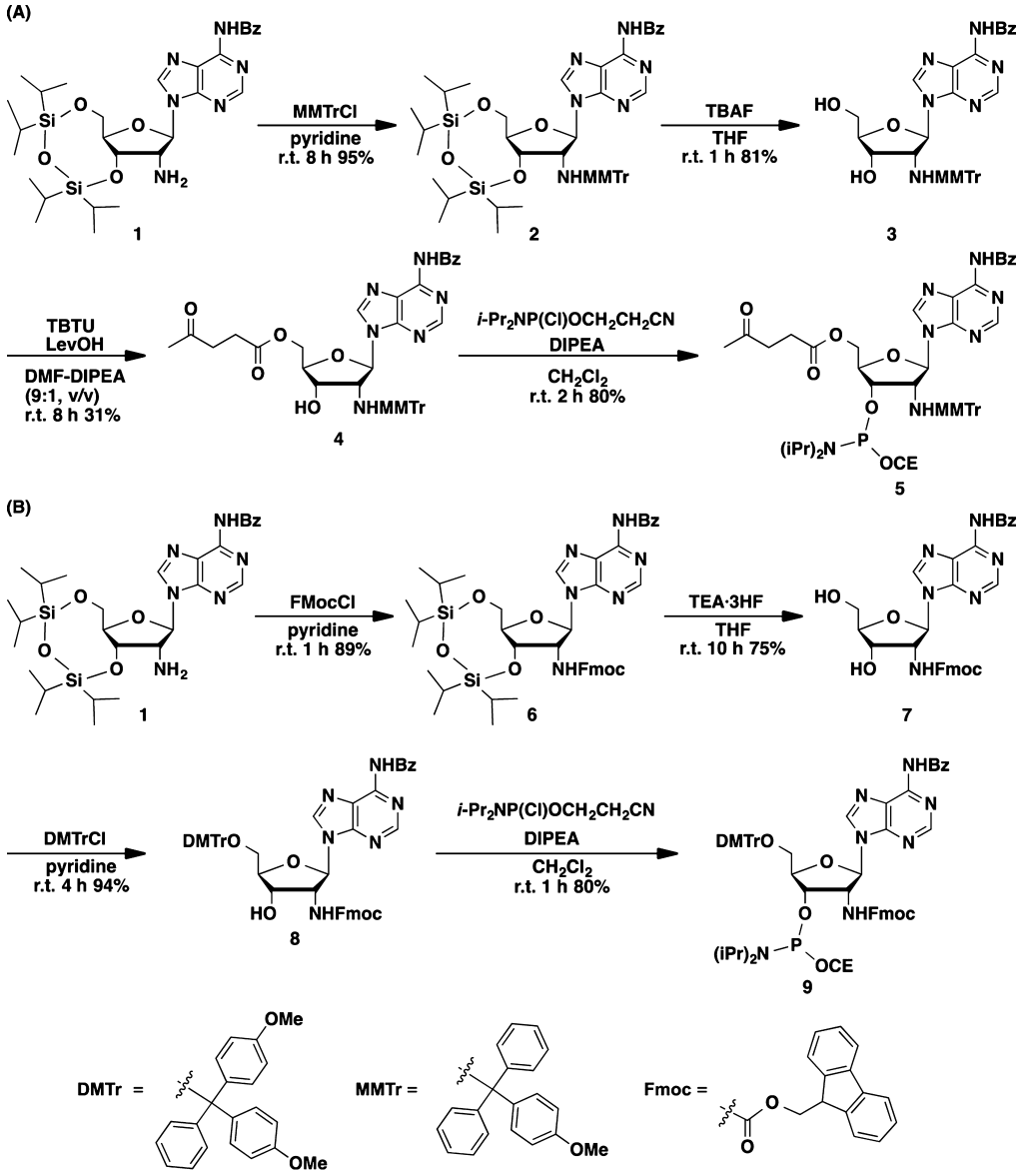

(Figure 2A and Figure 3A). Immediately after ETT activation (Figure 2A,ii), the signals corresponding to **5** at 148 and 152 ppm disappeared and were replaced by a signal at 174 ppm. The same signal was also found in the DCI treated sample together with a signal from the starting material at 152 ppm (Figure 2A,iii). We surmise that the signal of 174 ppm corresponds to a product of cyclization of **5** (Figure 2B, **5-A**) that is prompted by a nucleophilic attack of the 2′-amino nitrogen onto the activated, electrophilic 3′ phosphorus center. In this reaction, the activated intermediate was immediately attacked by the 2′-amino nitrogen so that the activated signal was not detectable by ^{31}P NMR. Surprisingly, this cyclic product (**5-A**) displayed notable stability in the presence of excess ethanol even after 24 h (Figure S1). The ETT-activated cyclization was found to be significantly faster than with DCI activation.

In the presence of activating agents, ETT and DCI, the 2′-*N*-Fmoc amidite **9** was rapidly transformed into a mixture of products, as indicated by the new ^{31}P NMR signals detected at 129 and 8 ppm (Figure 3A,ii, iii). However, the signal at 8 ppm, which is expected as hydrolyzed product was the major product in all cases. We hypothesize that the signal at 129 ppm corresponds to 2′,3′ cyclic structure **9-A** (Figure 3B) or, alternatively, a 2′,3′ cyclic structure resulting from nucleophilic attack by the oxygen carbonyl (Fmoc moiety) rather than the 2′-nitrogen.[25] Additionally, the cyclic product exhibited stability against nucleophilic attack after treatment with excess ethanol for >24 h (Figure S2). The formation of cyclized products in the presence of ETT and DCI potentially precludes the use of amidites **5** and **9** in coupling reactions, particularly in the case of **5** since the 2′,3′-cyclic product may be incapable of reacting with the 5′ hydroxyl of a growing oligonucleotide chain or may create an isomerized product. Consequently, we repeated those experiments in the presence of preadded ethanol to simulate a coupling reaction. Under these conditions, the 2′-*N*-Fmoc (**9**) compound resisted cyclization to **9-A** relative to the 2′-*N*-MMTr compound (**5**), presumably the result of reduced nucleophilicity due to dispersion of the nitrogen lone pair into the carbamate moiety. The 2′-*N*-MMTr compound can attack the phosphorus of the activated vicinal phosphoramidite species

DOI: 10.1021/acs.joc.5b01719
J. Org. Chem. 2015, 80, 10108−10118

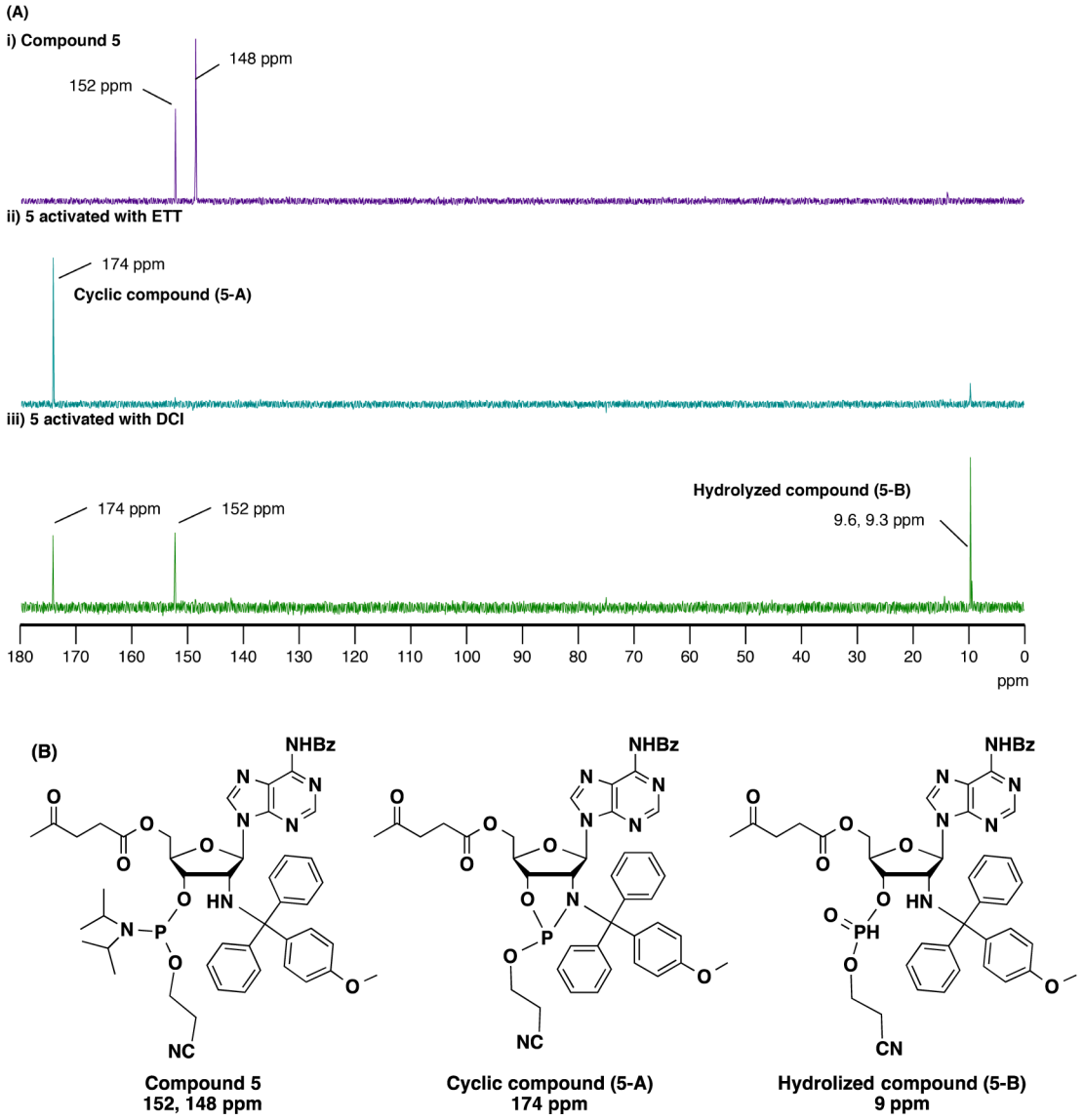

Figure 2. (A) ^{31}P NMR spectra of compound **5** under the coupling conditions. (i) Compound **5**, (ii) compound **5** activated with ETT, and (iii) compound **5** activated with DCI. (B) Proposed structure of compound corresponds to the NMR peaks.

regardless of its steric effect and thereby compete with the alcohol intended for that role, while the 2′-*N*-Fmoc is exclusively the target of an alcohol and thereby converted to the desired phosphite triester compound (Figure S3). Consequently, due to its chemical instability under standard coupling conditions, we dismissed the MMTr-protected amidite **5** and engaged in solid-phase bRNA synthesis with Fmoc-protected branching amidite **9** only.

Branch RNA Synthesis on Solid Support. Four 2′ phosphoramidate-linked branched RNA molecules (bN-RNAs) were synthesized, each consisting of a dinucleotide or pentanucleotide joined at a branchpoint adenosine unit (Table 1). Sequences of bN-RNAs **2**–**4** are variations on the sequence of the native yeast *rp51* intron branchpoint. Syntheses of these were performed on an automated DNA synthesizer using a controlled-pore glass solid support and ETT as an activator. In a first step, standard 2′-*O*-TBDMS, 5′-*O*-DMTr, 3′-*O*-phosphoramidite building blocks (S: standard 3′-*O*-phosphoramidite monomer) were coupled in order to grow the first 3′,5′ branch of the desired sequence (Scheme 2). The branchpoint monomer (**9**) was then incorporated through standard coupling conditions, and the cycle was resumed to extend the 5′-branch segment using commercially available monomers. With ETT as an acid activator, coupling of (**9**) proceeds in 60−80% efficiency as assessed by the trityl assay method. Next, the 5′ terminus of the branch was detritylated and capped (Ac_2O) to prevent further extension of this segment. Prior to deblocking the 2′-*N*-Fmoc at the branchpoint, all cyanoethyl groups were removed from the internucleotidic phosphotriesters with a TEA/MeCN treatment (room temperature, 90 min). The resulting phosphodiesters are then stable against nucleophilic attack by the deprotected 2′ amino nitrogen on the vicinal 3′ phosphates, a reaction that would lead to subsequent 3′-to-2′-phosphate migration or chain cleavage. Next, the 2′-*N*-Fmoc group was efficiently cleaved with 4-methylpiperidine in DMF (room temperature, 15 min). Finally, the remaining 2′-branch segment was generated in the reverse 5′-3′ direction using commercially available 2′-*O*-TBDMS, 3′-*O*-DMTr, 5′-*O*-phosphoramidite RNA monomers (R: reverse 5′-*O*-phosphoramidite monomer). To minimize

DOI: 10.1021/acs.joc.5b01719
J. Org. Chem. 2015, 80, 10108−10118

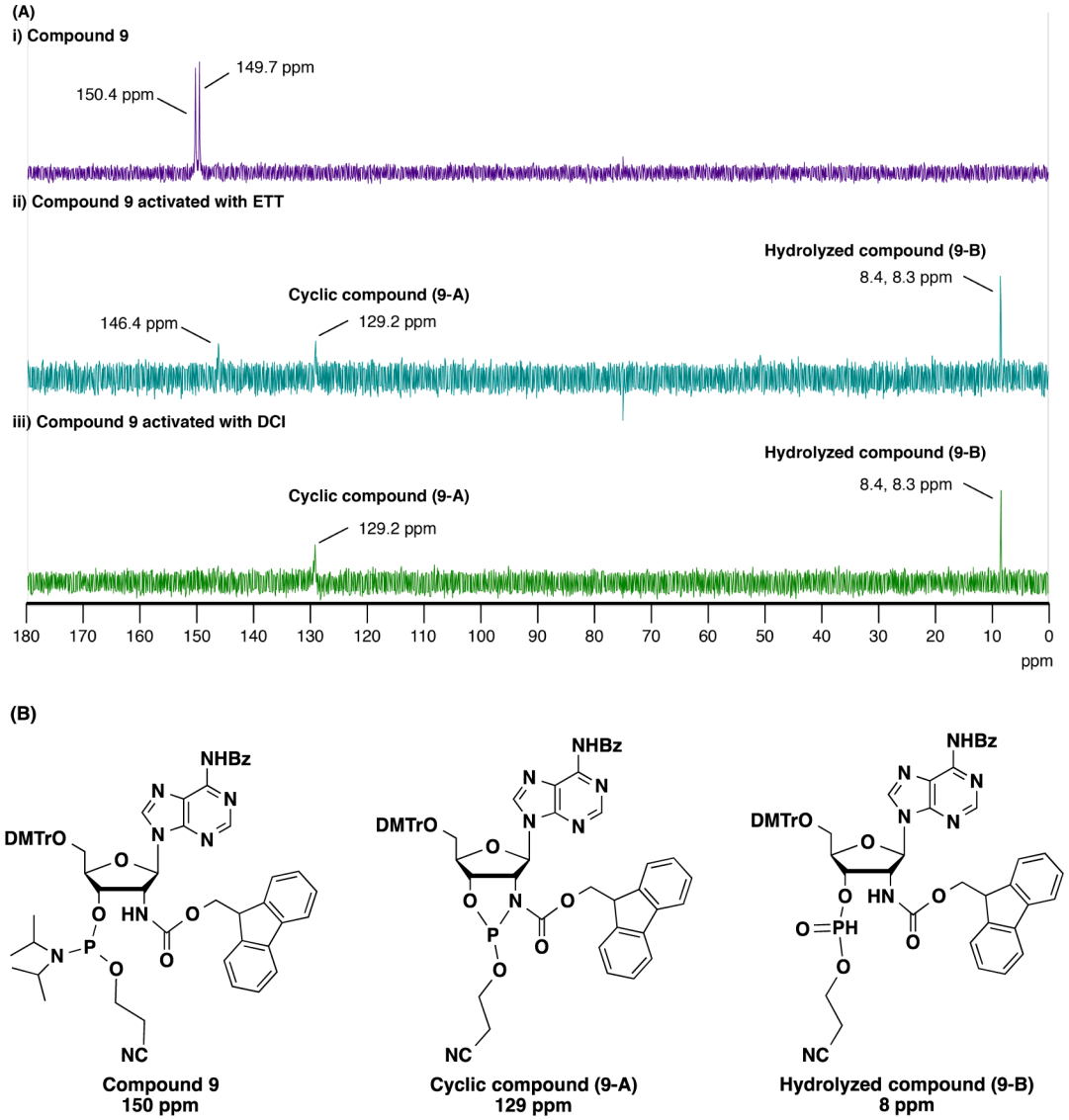

Figure 3. (A) ^{31}P NMR spectra of compound **9** under the coupling conditions. (i) Compound **9**, (ii) compound **9** activated with ETT, and (iii) compound **9** activated with DCI. (B) Proposed structure of compound corresponds to the NMR peaks.

Table 1. List of Branched RNAs Synthesized in This Study

entry	molecule	sequence (5′-3′)	isolated nmol[a]	calculated mass	observed mass
1	bN-RNA1[b]	TTTTTA(2′-*N*-TTTTT)TTTTT	37	4826.8	4826.7
2	bN-RNA2	UAA(2′-*N*-GU)CA	52	2186.4	2186.3
3	bN-RNA3	UACUAA(2′-*N*-GUGUG)CAAGU	8.4[c]	5102.7	5102.7
4	bN-RNA4	UACUAA(2′-*N*-GUAUG)CAAGU	28[d], 31[e]	5088.7	5088.8

[a]The synthesis scale was 1 μmol, and ETT was used an activator for all entries. [b]T in the sequence represents thymidine. [c]TEA·3HF was used as a desilylating reagent. [d]TBAF in THF was used as a desilylating reagent. [e]TEA·3HF/NMP/TEA was used as a desilylating reagent.

steric effects at the 2′ branching position, a doubled coupling time and concentration (30 min and 0.3 M respectively) was necessary to accelerate the coupling reaction of the first reverse monomer. Deprotection was then performed stepwise, first with 33% ammonia−ethanol (4:1, v/v) treatment (room temperature, 48 h) followed by desilylation with TEA·3HF (room temperature, 48 h). Due to the reported acid-labile nature of phosphoramidite linkages,[26] alternative desilylation reagents have been considered such as TBAF in THF and TEA·3HF in 1-methyl-2-pyrrolidinone (NMP) and triethylamine (TEA). The desilylation with nonacidic desilylating reagents afforded better bRNA yields (Table 1). Purification then proceeded first through anion-exchange high-performance liquid chromatography (HPLC) and subsequently through 24% poly acrylamide gel electrophoresis (PAGE). Employing this strategy, three bN-RNA sequences were generated in modest yields (Table 1) and tested in chemical and biological assays.

Chemical Stability of the 2′,5′ Phosphoramidate Linkage. In order to investigate the stability of the novel 2′,5′ phosphoramidate linkages, synthetic bRNA sequences were exposed to various acidic, basic, and fluoride conditions.

DOI: 10.1021/acs.joc.5b01719
J. Org. Chem. 2015, 80, 10108−10118

Scheme 2. Divergent Synthesis of 2′,5′ Phosphoramidate-Linked bRNA Employing Monomer 9 at the Branchpoint

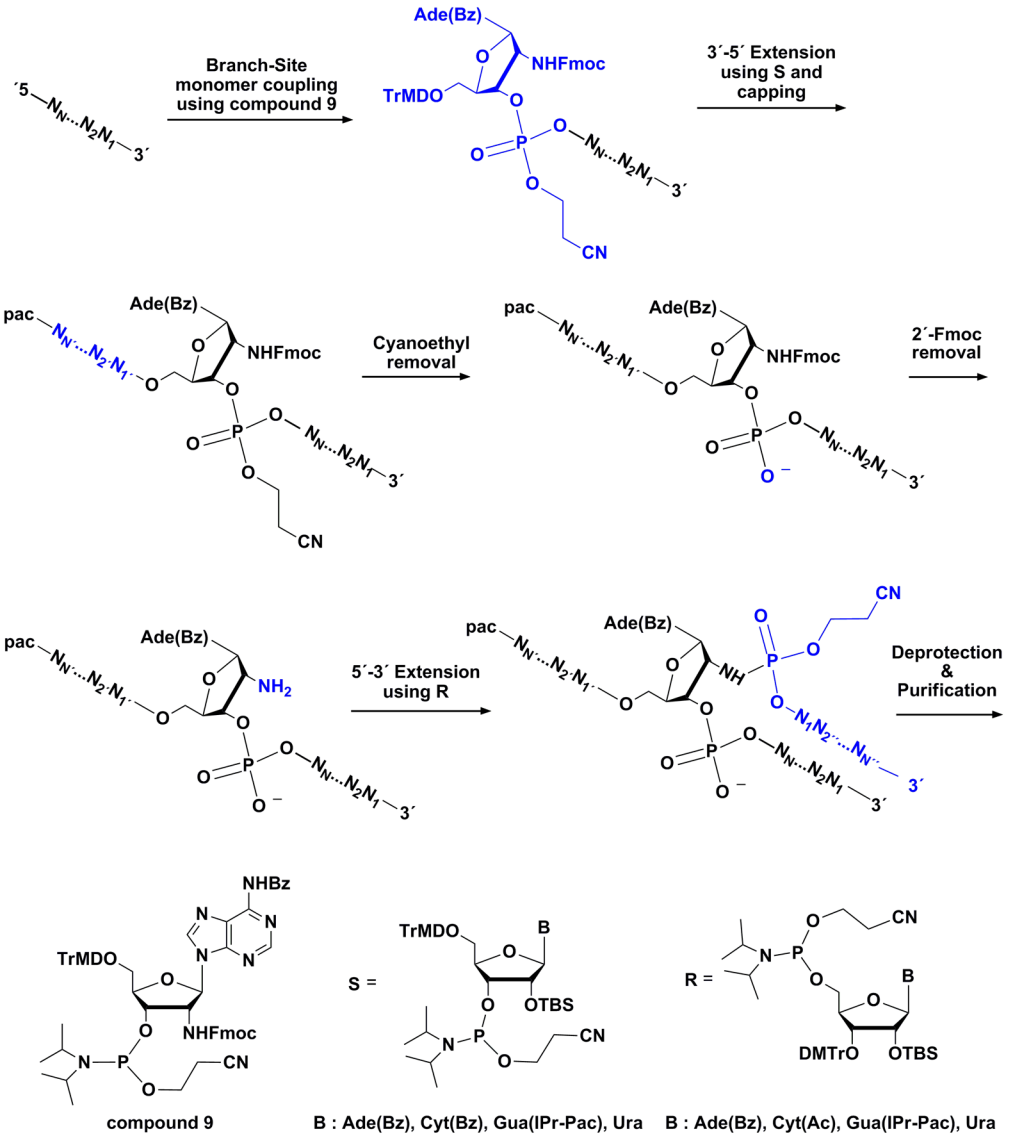

To clearly assess the stability of the modified branchpoint linkage during solid-phase synthesis, we selected bN-RNA1 as a model sequence considering the chemical inertness of its DNA branches. The results were evaluated by ion-exchange HPLC (Figure S4) and revealed a strong resistance to various basic treatments, particularly those that are commonly used during oligonucleotide cleavage from the solid support, cyanoethyl removal, and base deprotection. Conversely, exposing bN-RNA1 to acidic conditions (40% acetic acid, room temperature, 24 h) resulted in nearly 50% hydrolysis. Indeed, the exposure of bN-RNA1 to TEA·3HF (65 °C, 3 h) resulted in the complete and selective hydrolysis of the branchpoint phosphoramidate linkage. However, in neutralized fluoride-containing desilylation conditions, bN-RNA1 did not degrade (Figure 4). These results further highlight the need for optimizing desilylation conditions to improve bRNA synthesis yields (Table 1, conditions b vs c/d).

Susceptibility of bN-RNA to Debranching Enzyme. In order to assess the compatibility of the 2′ phosphoramidate bRNAs as a substrate for Dbr1 2′,5′ debranching, the modified bN-RNA4 and the equivalent 2′-phosphodiester bRNA5 were ^{32}P-radiolabeled at their 5′ terminus. The debranching reaction was monitored in the presence of 0.5 μM of Dbr1, and the products separated by PAGE and visualized by autoradiography. (Figure 5). These results revealed that the unmodified bRNA5 underwent debranching within seconds, while some of bN-RNA4 still remained after 60 min.

Inhibition Assays. Synthetic bN-RNAs were evaluated for their ability to attenuate Dbr1 enzymatic activity. The reaction rate was monitored using a ^{32}P-labeled natural bRNA substrate (bRNA5). The debranching reactions were carried out in the presence of either phosphoramidate-modified bN-RNA2 or bN-RNA4. RNA6, a linear control lacking the 2′ branch segment, was used as a negative control. To perform those inhibition assays, bN-RNA2, bN-RNA4, and RNA6 were added to solutions containing Dbr1 (20 nM) at increasing concentrations in order to assess their effect on Dbr1 activity. For RNA6 and bN-RNA2, the concentrations were varied from 0 to 10 μM. On the other hand, for bN-RNA4, the concentrations were varied from 0 to 0.5 μM, as the attenuation of Dbr1 activity was greater than that of RNA6 and bN-RNA2.

DOI: 10.1021/acs.joc.5b01719
J. Org. Chem. 2015, 80, 10108−10118

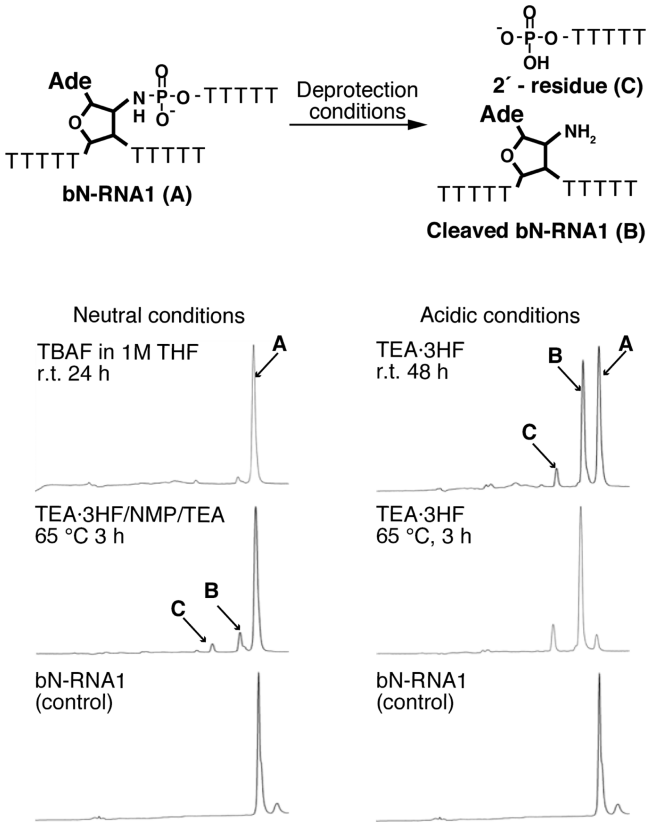

Figure 4. Ion-exchange chromatographs of bN-RNA1 after exposure to several deprotection conditions.

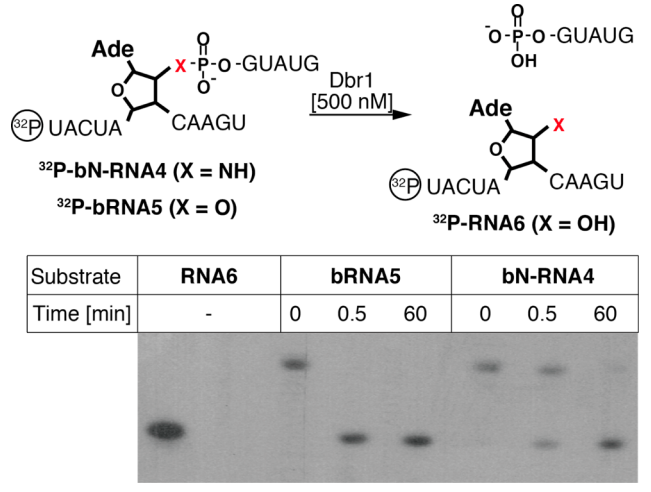

Figure 5. (A) Schematic procedure of stability to debranching enzyme. (B) PAGE result of the procedure; bN-RNA4 or bRNA5 (5 μM each) following 0.5 and 60 min time points. The first lane features a ^{32}P-labeled synthetic product control (RNA6).

The debranched products were separated by PAGE and visualized by autoradiography (Figures 6 and S5–S7).

Analysis of the densitometry data clearly indicated that increasing amounts of bN-RNA2 or bN-RNA4 slowed down the activity of Dbr1 (Figure 6B), while the single strand negative control (RNA6) showed no significant effect at any of the tested concentrations (Figure S7). The IC_{50} value of bN-RNA4 is estimated to be ~40 nM from analysis of the dose–response curve. The data also suggested that the larger 16mer

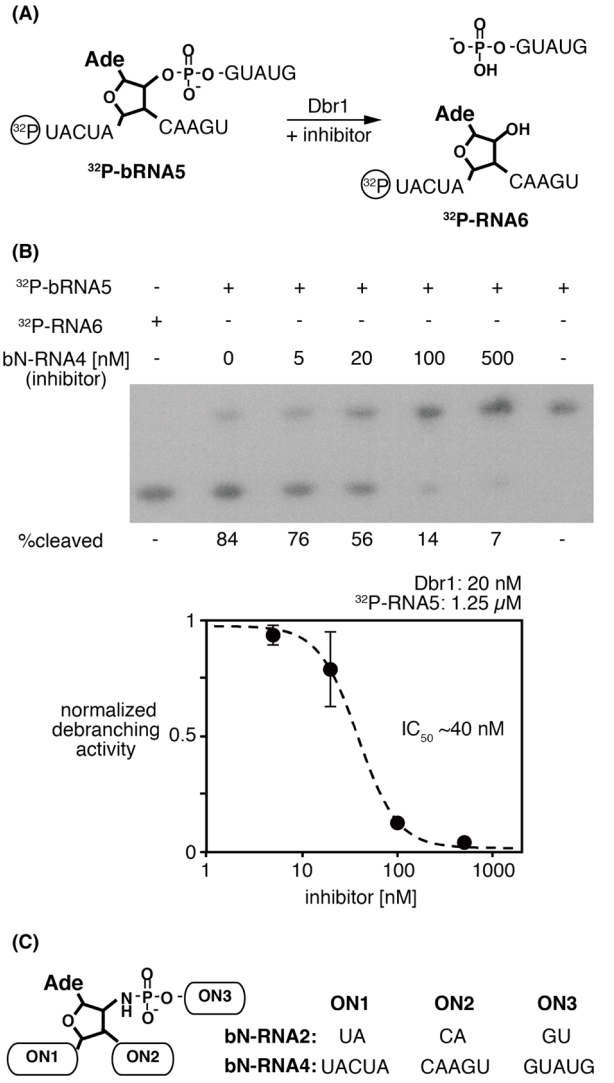

Figure 6. (A) Schematic representation of the inhibition assay. (B) Products of reaction of Dbr1 + ^{32}P-bRNA5 as a function of increasing concentrations of bN-RNA4. (C) The structure of bN-RNA2 and bN-RNA4.

bN-RNA4 is more potent than the heptamer (bN-RNA2) sequence (Figures S5 and S6). This is fully consistent with crystal structures of bRNA:Dbr1 in which 5 nucleotides of the 2′-arm of the bRNA are observed contacting Dbr1 (Clark, Katolik *et al.*, to be published). Hence, those bRNAs possessing only 2 nucleotides in the 2′-arm (e.g., bN-RNA2) might have a faster off-rate (or slower on-rate) than those with 5 nucleotides in that arm (e.g., bN-RNA4). Overall, our results suggest that the 16mer (bN-RNA4) sequence binds more strongly to Dbr1 than the shorter sequence (bN-RNA2).

Given that bN-RNA2 and bN-RNA4 are processed slowly by their target enzyme, they might be better described as pseudosubstrate inhibitors or alternate substrate inhibitors.[27] *A priori*, the on- and off-rates for the nearly identical wild-type and P-amidate bRNAs (e.g., bRNA6 vs bN-RNA4) should be the same, as substituting a 2′-O with a 2′-N on the scissile phosphate is not expected to significantly alter those parameters; in fact, the only part of Dbr1 interacting with the 2′-N is His91[13] (Figure 1). Hence, we postulate that the inhibition observed in the presence of the bN-RNAs probably

DOI: 10.1021/acs.joc.5b01719
J. Org. Chem. 2015, 80, 10108–10118

comes from the "slow" hydrolysis step in the P-amidate linkage compared to the wild-type phosphodiester bond.

CONCLUSIONS

This study is the first to report the synthesis of a bRNA containing a 2′,5′ phosphoramidate linkage (bN-RNA). We have successfully prepared a branchpoint nucleotide building block for the development of modified bN-RNAs with 2′,5′ phosphoramidate linkages. We have evaluated both the 2′-*N*-Fmoc and 2′-*N*-MMTr groups to protect the 2′ amino function during solid-phase synthesis of the bN-RNAs. ^{31}P NMR spectroscopy indicated that both branch monomers underwent cyclization under coupling conditions, but the 2′-*N*-Fmoc protected monomer seemed to cyclize to a much lower rate and was consequently deemed suitable for solid-phase synthesis. The resulting synthetic bN-RNAs were additionally tested for their stability under DNA/RNA deprotection conditions. It was found that the 2′,5′ phosphoramidate linkage at the branchpoint was acid labile and consequently hydrolyzed in the acidic fluoride-containing desilylation mixtures required for 2′-*O*-TBDMS removal. However, the use of desilylation solutions at neutral pH significantly improved the total recovery yield of bN-RNA synthesis. The bN-RNAs were tested as substrates for the Debranching Enzyme (Dbr1). While the 2′-5′ phosphoramidates were substrates for Dbr1, they are significantly more resistant to the action of the enzyme than the natural bRNAs of identical sequence. Finally, the 2′ phosphoramidate-linked bRNAs were evaluated for their ability to inhibit Dbr1, an effect that may be applicable in work seeking to reduce the toxicity of TDP-43 involved in ALS.

Since complete inhibition of debranching activity is lethal,[28] care must be taken to design inhibitors with very specific pharmacological properties. The structures presented in this work may help guide such efforts since, theoretically, there could be a benefit in using an alternate substrate inhibitor over a full inhibitor as a therapeutic agent. That is, a slowly hydrolyzed alternate substrate inhibitor would permit a spike of intron lariats to accumulate (and sequester existing TDP-43 pool), and upon hydrolysis of the alternate inhibitor, "normal" Dbr1 activity would be restored. We believe our results will help guide the rational design of inhibitors that may represent novel therapeutic agents to treat neurodegenerative disease.

EXPERIMENTAL SECTION

General Information. All chemicals were purchased from commercial sources and were used as received. Where required, solvents were dried on molecular sieves (4 Å) overnight.

Solid Phase Synthesis of Branched RNAs. *Materials and Reagents.* Branched RNAs were synthesized using DNA/RNA synthesizer (ABI) on a 1 μmol scale of unilink support CPG resin (ChemGenes, 22 μmol/g). Conventional and reverse 2′ TBDMS and bis-cyanoethyl-*N*,*N*-diisopropyl phosphoramidite were used (0.15 M in MeCN). Dissolved phosphoramidites were activated with required activator (5-ethylthio-1*H*-tetrazole (ETT) or 4,5-dicyano imidazole (DCI) (0.25 M in MeCN)). ETT was used for the synthesis all bN-RNAs shown in Table 1. Capping was carried out following every coupling reaction by the simultaneous delivery of acetic anhydride in pyridine/THF and *N*-methylimidazole (16% in THF) and contacting the solid support for 6 s. Oxidation of phosphite triester intermediates was carried with 0.1 M iodine in pyridine/H_2O/THF (20 s). A solution of 3% trichloroacetic acid in THF, delivered over 1.8 min, was used to deblock DMTr groups. After elongation toward 3′ to 5′, cyanoethyl (CNEt) phosphate was deprotected using anhydrous triethylamine/MeCN (2:3, v/v) over 1.3 h. Fmoc protection on 2′-amino of branch site was cleaved using 10% 4-methylpiperidine in anhydrous DMF over 15 min. Oligonucleotides were deprotected and cleaved from the solid support using NH_4OH:EtOH (3:1, v/v) or concentrated ammonium hydroxide solution. Then TBDMS groups were cleaved with TEA·3HF-NMP-TEA (3:2:3, v/v/v) at 65 °C for 3 h or 1 M TBAF in THF at ambient temperature for 8 h.

Purification of bRNAs. Synthesized compounds were purified by HPLC using an anion-exchange column (Protein PAK DEAE 5PW 21.5 mm × 15 cm). The buffer system consisted of water as solution A and 1 M aqueous lithium perchlorate as solution B at a flow rate of 4 mL/min. The gradient was 0−40% of buffer B over 50 min at 60 °C. The desired peak was collected and then desalted using a pre-eluted size exclusion column filled with NAP-25 matrix. The column was eluted with sterile water and 7 × 1 mL fractions were collected. Each fraction was quantified by absorbance (λ = 260 nm). Analytical PAGE was used to assess the quality of purified products, and additional preparative polyacrylamide purification of bRNAs was performed as needed. The mass of each purified compound was confirmed by ESI-TOF.

Analytical HPLC. The crude or purified samples were analyzed by anion-exchange column (Protein DEAE 5PW 7.5 × 75 mm). The buffer system was the same as purification. The gradient was 0−24% of buffer B over 30 min at 65 °C.

Radio-Labeling of the bRNA Samples. (Warning: caution must be taken with ^{32}P, including shielding, decontamination, and respecting CNSC or other local radiation safety regulations.) In a 20 μL total volume, bRNA (100 pmol, 5 μM) was incubated with γ-^{32}P-ATP (50−150 μCi), 2000 units T4 polynucleotide kinase in 70 mM Tris-HCl pH 7.6, 10 mM $MgCl_2$, and 5 mM DTT. After incubation at 37 °C for 1 h, a NAP-10 column equilibrated in water was used to remove unincorporated γ-^{32}P-ATP from labeled bRNA. The resulting samples were dried down, and activity quantitated. The size exclusion column provided a rough separation of labeled oligonucleotide (which eluted in second, third, and fourth fractions) from the free γ-^{32}P-ATP (which eluted in subsequent fractions).

^{32}P Autoradiography Assays. (Warning: caution must be taken with ^{32}P, including shielding, decontamination, and respecting CNSC or other local radiation safety regulations.) 12% (19:1) polyacrylamide gels in 7 M urea and 1× TBE (89 mM tris base, 89 mM boric acid, 2 mM EDTA) were used in both debranching and inhibition assays. For each lane in the gel, approximately 100−1000 microcuries of labeled RNA were loaded. The running buffer contained 0.5× TBE buffer (44.5 mM tris base, 44.5 mM boric acid, 1 mM EDTA), and samples were electrophoresed at 1000 V for 3 h. X-ray film was placed on each gel and exposed overnight and developed using commercial developer and fixer solutions.

Debranching Assays. Reactions were carried out in a 20 μL total volume and a 10:1 substrate enzyme ratio. The reactions contained: the substrate (bN-RNA4 or bRNA5 (5 μM) + respective ^{32}P-bN-RNA4 or ^{32}P-bRNA5 (low nM, 1000−20,000 cpm)), Dbr1 (0.5 μM), NaCl (100 mM), HEPES (10 mM, pH 7.0−7.6), tris(2-carboxyethyl)-phosphine (0.5 mM), and Tween20 (0.005% v/v). Specifically, a 9 μL mixture containing the substrate was added to 10 μL of the 2× salt buffer, and the reactions were initiated by adding 1 μL of Dbr1 (10 μM). Unlabeled substrate was mixed with the 5′-^{32}P substrate because the exact concentration of radiolabeled substrates was not precisely established. Therefore, a known and much greater concentration of matching unlabeled bRNA was added to each labeled bRNA, and the concentration of unlabeled bRNA used as a surrogate for the total substrate concentration. The reaction was analyzed at two time points (30 s and 1 h). Each time 10 μL of the reaction mixture was withdrawn, added to 14 μL of deionized formamide gel loading buffer to stop the reaction, and immediately frozen in solid CO_2. Next, the samples were heated to 95 °C for 5 min and loaded onto a 12% polyacrylamide gel and developed as described above. Synthetic ^{32}P-RNA6 was run as a control to verify that the correct debranched product was being formed.

Dbr1 Inhibition Assays. Reactions were carried out in a 10 μL total volume and a 62.5:1 substrate:enzyme ratio. The reaction mixture contained: Dbr1 (20 nM), NaCl (100 mM), HEPES (10 mM, pH 7.0−7.6), tris(2-carboxyethyl)phosphine (0.5 mM), Tween20 (0.005%

DOI: 10.1021/acs.joc.5b01719
J. Org. Chem. 2015, 80, 10108−10118

v/v), BSA (0.05 mg/mL), substrate (bRNA5 (1.25 μM) + ^{32}P-bRNA5 (estimated <0.2 μM, 100−1000 cpm)), and the bN-RNA inhibitor (conc. specified in Figure 6). More specifically, the reactions were initiated by combining 5 μL of a freshly thawed (−80 °C to rt) aliqot containing Dbr1 (40 nM), NaCl (200 mM), HEPES (20 mM pH 7.0−7.6), tris(2-carboxyethyl)phosphine (1 mM), Tween20 (0.01% v/v), and BSA (0.1 mg/mL) with 5 μL of a mixture containing the inhibitor (twice the final reaction concentration) and the substrate (bRNA5 (2.5 μM) + ^{32}P-bRNA5 (estimated <0.4 μM). Following initiation, the reactions were constantly mixed for the first 30 or 60 s by pipetting. Following an additional period (30 s or 1 min), 5 μL aliquots of the reaction mixtures were removed, added to 7 μL of deionized formamide gel loading solution to stop the reaction, and immediately frozen. Next, the samples were together heated to 95 °C for 5 min, loaded onto a 12% polyacrylamide gel, and developed as above. On the same gel, a parallel lane was supplemented with synthetic ^{32}P-RNA6 to serve as a control for the expected product of debranching. The developed X-ray films were scanned and densitometrically analyzed by the program ImageJ64. Next, the % cleavage value was obtained from each lane by dividing the density (quantity of radiation) of hydrolyzed product by the sum of the density of the substrate and product. This ratio was then normalized so that 100% represented the uninhibited reaction, and this allowed the averaging of two assays. Finally, the values were plotted into Graphpad Prism, which fitted a curve and obtained the IC_{50} for bN-RNA4.

^{31}P NMR Study of Compounds 5 and 9. 40 mg of each nucleoside was dissolved in 400 μL of dried deutrated acetonitirile. A required activator such as 4,5-dicyano imidazole (DCI) or 5-ethylthio-1*H*-tetrazole (ETT) was added to make the solution 0.25 M, which is the normal procedure in a DNA/RNA coupling method. Those procedures were done in a NMR tube.

*N^6-Benzoyl-2′-deoxy-2′-amino-3′,5′-O-[1,1,3,3-tetrakis(1-methylethyl)-1,3-disiloxanediyl]adenosine (**1**).* The compound was synthesized according to previously published protocols.[24]

*N^6-Benzoyl-2′-deoxy-2′-[(4-methoxytrityl)amino]-3′,5′-O-[1,1,3,3-tetrakis(1-methylethyl)-1,3-disiloxanediyl]adenosine (**2**).* Compound **1** (1.70 mg, 2.78 mmol) was co-evaporated with dried pyridine for 3 times, then dissolved in dried pyridine (27.8 mL), and the reaction was stirred at ambient temperature under argon. Next, 4-methoxytrytyl chloride (1.028 g, 3.33 mmol) was added into the flask. After 8 h, CH_2Cl_2 and $NaHCO_3$ (sat. aq.) were added. The organic phase was washed three times with $NaHCO_3$ and once with brine. The combined aqueous layers were extracted with CH_2Cl_2 once. The combined organic layers were dried over Na_2SO_4, filtered, and concentrated. The residue was purified by flush column chromatography (SiO_2, 3:7 hexane/ethyl acetate) to yield compound **3** (2.348 g, 95%) as an amorphous yellow solid: ^{1}H NMR (400 MHz, acetonitrile-d_3) δ 9.21 (s, 1H), 8.46 (s, 1H), 7.99 (d, *J* = 7.6 Hz, 2H), 7.70−7.59 (m, 2H), 7.60−7.51 (m, 2H), 7.46−7.35 (m, 4H), 7.26−7.07 (m, 8H), 6.65 (dt, 2H), 5.34 (d, *J* = 3.5 Hz, 1H), 4.71 (t, *J* = 6.6 Hz, 1H), 4.31 (dt, *J* = 6.8, 3.5 Hz, 1H), 4.21 (td, *J* = 6.3, 3.2 Hz, 1H), 3.94 (dd, *J* = 12.4, 3.3 Hz, 1H), 3.79 (dd, *J* = 12.4, 6.1 Hz, 1H), 3.72 (d, *J* = 3.5 Hz, 1H), 3.69 (s, 3H), 1.22−0.90 (m, 28H); ^{13}C NMR (101 MHz, acetonitrile-d_3) δ 159.2, 152.5, 147.8, 147.4, 144.6, 138.5, 133.5, 131.1, 129.7, 129.4, 129.2, 129.0, 128.9, 128.8, 127.6, 127.5, 125.8, 118.3, 114.0, 90.2, 84.5, 72.2, 70.9, 63.1, 59.1, 55.8, 17.8, 17.6, 17.6, 17.5, 17.4, 14.3, 13.9, 13.9, 13.7, 1.9, 1.9, 1.8, 1.7, 1.6, 1.7, 1.5, 1.4, 1.4, 1.3, 1.2, 1.2, 1.1, 1.0, 1.0, 0.9, 0.8, 0.7, 0.6; HRMS (ESI Q-TOF) *m*/*z*: [M + Na]$^+$ calcd for $C_{49}H_{60}N_6O_6Si_2Na$ 907.4005; found 907.3990.

*N^6-Benzoyl-2′-deoxy-2′-[(4-methoxytrityl)amino]adenosine (**3**).* Compound **2** (2.15 mg, 2.4 mmol) was dissolved in THF (6.4 mL), and the reaction was stirred at ambient temperature under argon. 1 M TBAF in THF (5.6 mL, 5.6 mmol) was then added into the flask. After 1 h, silicagel (SiO_2, 7.5 g) was added to quench the excess of TBAF. The mixed solution was concentrated and then directly loaded on a flush column chromatography (SiO_2, 1:1 to 1:9, hexane/ethyl acetate) to yield compound **3** (1.25 g, 81%) as a white solid: ^{1}H NMR (500 MHz, chloroform-*d*) δ 9.14 (s, 1H), 8.61 (s, 1H), 8.25 (s, 1H), 8.08 (d, 2H), 7.65 (t, *J* = 7.5 Hz, 1H), 7.57 (t, *J* = 7.6 Hz, 2H), 7.19 (dd, 4H), 7.12−6.96 (m, 6H), 6.60 (d, *J* = 8.9 Hz, 1H), 5.84 (d, *J* = 12.1, 2.1 Hz, 1H), 5.78 (d, *J* = 8.9 Hz, 1H), 4.13 (q, *J* = 9.2, 8.7 Hz, 1H), 4.06 (s, 1H), 3.80 (d, *J* = 12.9 Hz, 1H), 3.70 (s, 3H), 3.45 (t, *J* = 12.5 Hz, 1H), 2.90 (t, *J* = 4.5 Hz, 1H), 2.79 (d, *J* = 10.7 Hz, 1H), 1.65 (s, 4H), 1.50 (d, *J* = 4.3 Hz, 1H). ^{13}C NMR (126 MHz, chloroform-*d*) δ164.5, 158.3, 152.2, 150.9, 150.3, 146.1, 146.0, 143.4, 137.8, 133.6, 133.1, 129.5, 129.1, 128.1, 128.1, 128.0, 128.0, 128.0, 126.9, 124.9, 113.4, 109.9, 92.0, 88.7, 77.4, 77.2, 76.9, 71.3, 69.8, 63.5, 60.0, 55.3.; HRMS (ESI Q-TOF) *m*/*z*: [M + Na]$^+$ calcd for $C_{37}H_{34}N_6O_5Na$ 665.2483; found 665.2481.

*N^6-Benzoyl-2′-deoxy-5′-O-levulinyl-2′-[(4-methoxytrityl)amino]-adenosine (**4**).* TBTU (889 mg, 2.77 mmol) was dissolved in DMF (8.28 mL) and *N*,*N*-diisopropylethylamine (0.92 mL) and stirred at room temperature under argon. Freshly distilled levulinic acid (281 μL, 2.77 mmol) was added, and the reaction was stirred at room temperature for 30 min. Compound **3** (594 mg, 0.92 mmol) was dried under a vacuum in a flask with a magnetic stirrer. The solution of TBTU/levulinic acid reaction was added dropwise for 10 min to the nucleoside and stirred at room temperature for 8 h. Next, CH_2Cl_2 and $NaHCO_3$ (sat. aq.) were added, and the mixture was separated. The organic phase was washed three times with $NaHCO_3$. The combined aqueous layers were extracted once with CH_2Cl_2. Next, the combined organic extracts were washed once with brine and subsequently combined with the original organic layer, dried with Na_2SO_4, filtered, and concentrated. The residue was purified by column chromatography (SiO_2, 1:1 → 1:9 hexane/ethyl acetate) to yield compound **4** (194 mg, 31%) as an amorphous white solid: ^{1}H NMR (400 MHz, DMSO-d_6) δ 11.27 (s, 1H), 8.70 (s, 1H), 8.58 (s, 1H), 8.14−8.06 (m, 2H), 7.66 (d, *J* = 7.3 Hz, 1H), 7.58 (t, *J* = 7.6 Hz, 2H), 7.29−7.02 (m, 12H), 6.65 (d, *J* = 8.8 Hz, 2H), 6.10 (d, *J* = 8.6 Hz, 1H), 5.51 (d, *J* = 3.9 Hz, 1H), 4.15−3.87 (m, 4H), 3.66 (s, 3H), 3.11 (d, *J* = 10.0 Hz, 1H), 2.68 (t, *J* = 6.5 Hz, 2H), 2.43−2.34 (m, 2H), 2.16 (t, *J* = 4.2 Hz, 1H), 2.09 (s, 3H); ^{13}C NMR (101 MHz, chloroform-*d*) δ 206.6, 172.4, 158.4, 152.7, 152.2, 145.9, 142.4, 137.5, 133.0, 130.0, 129.5, 129.1, 128.2, 128.1, 128.0, 126.9, 113.4, 113.4, 92.1, 88.8, 83.7, 77.5, 77.4, 77.3, 77.2, 76.8, 71.3, 70.5, 70.1, 64.3, 60.5, 58.1, 55.4, 53.6, 38.0, 31.1, 30.0, 27.9, 8.2, 1.3, 1.2.; HRMS (ESI Q-TOF) *m*/*z*: [M + Na]$^+$ calcd for $C_{42}H_{40}N_6O_7Na$ 763.2851; found 763.2841.

*N^6-Benzoyl-2′-deoxy-5′-O-levulinyl-2′-[(4-methoxytrityl)amino]-adenosine 3′-(2-cyanoethyl N,N-diisopropylphosphoramidite) (**5**).* Compound **4** (490 mg. 0.66 mmol) was dissolved in 6.6 mL CH_2Cl_2, and the mixture was stirred at 0 °C under argon. *N*,*N*-diisopropylethylamine (461 μL, 2.64 mmol) was added, followed by 2-cyanoethyl *N*,*N*-diisopropylchlorophosphoramidite (295 μL, 1.32 mmol), and then stirred at ambient temperature. After 2 h, CH_2Cl_2 and $NaHCO_3$ (sat aq) were added, and the mixture was separated. The organic phase was washed three times with $NaHCO_3$. The combined aqueous layers were extracted once with CH_2Cl_2. Next the combined organic extracts were washed once with brine and subsequently combined with the original organic layer, dried with Na_2SO_4, filtered, and concentrated. The residue was purified by column chromatography (SiO_2, 7:3 to 5:3, hexane/CH_2Cl_2). The fractions containing compound **4** were concentrated and then dissolved again with diethyl ether. The organic solvent was washed with $NaHCO_3$ four times to yield pure compound **5** (417 mg, 80%) as an amorphous white solid: ^{1}H NMR (500 MHz, chloroform-*d*) δ 9.11 (s, 1H), 8.70−8.54 (m, 1H), 8.17−8.12 (m, 1H), 8.06 (d, *J* = 7.7 Hz, 2H), 7.61 (t, *J* = 7.4 Hz, 1H), 7.53 (t, *J* = 7.6 Hz, 2H), 7.31−7.22 (m, 4H), 7.18−7.12 (m, 2H), 7.12−7.02 (m, 5H), 6.64−6.49 (m, 2H), 6.13−5.93 (m, 1H), 4.53−4.36 (m, 1H), 4.32 (t, *J* = 5.9 Hz, 1H), 4.21−4.09 (m, 2H), 3.70 (d, *J* = 3.0 Hz, 3H), 3.67−3.54 (m, 3H), 3.06 (d, *J* = 9.3 Hz, 1H), 2.99−2.90 (m, 1H), 2.77−2.65 (m, 2H), 2.60−2.23 (m, 4H), 2.20−2.14 (m, 3H), 1.98 (s, 1H), 1.16 (t, 12H).; ^{13}C NMR (126 MHz, chloroform-*d*) δ 206.7, 206.6, 172.5, 172.3, 164.7, 158.2, 152.6, 152.4, 152.2, 152.1, 149.6, 149.6, 146.2, 146.1, 143.5, 143.3, 137.8, 137.7, 134.0, 133.1, 132.9, 129.9, 129.7, 129.6, 129.4, 129.2, 129.0, 128.7, 128.4, 128.2, 128.0, 126.9, 126.6, 124.4, 124.3, 117.6, 114.0, 113.5, 113.1, 112.7, 89.8, 89.5, 82.9, 82.7, 82.0, 81.8, 77.5, 77.3, 77.0, 74.9, 74.8, 74.6, 74.5, 70.2, 70.1, 64.1, 59.0, 58.8, 58.6, 58.5, 56.0, 55.5, 55.4, 54.9, 44.1, 44.0, 43.6, 43.5, 43.1, 43.0, 38.0, 30.4, 30.2, 30.0, 29.8, 27.9, 27.8, 27.7, 25.4, 25.3, 25.2, 24.9, 24.8, 24.8, 24.7, 24.6, 20.4, 20.4, 20.2, 20.2, 20.0, 20.0.; 31P NMR (202

DOI: 10.1021/acs.joc.5b01719
J. Org. Chem. 2015, 80, 10108−10118

MHz, chloroform-*d*) δ 154.0, 151.1.; HRMS (ESI Q-TOF) *m*/*z*: [M + H]$^+$ calcd for $C_{51}H_{58}N_8O_8P$ 941.4110; found 941.4123.

*N^6-Benzoyl-2′-deoxy-2′-[(9-fluorenylmethyloxycarbonyl)amino]-3′,5′-O-[1,1,3,3-tetrakis(1-methylethyl)-1,3-disiloxanediyl]-adenosine (**6**).* Compound **1**(1.2 g, 1.96 mmol) was co-evaporated with dried pyridine for 3 times, then dissolved in dried pyridine (20 mL), and the reaction was stirred at ambient temperature under argon. Next, fluorenylmethyloxycarbonyl chloride (556 mg, 2.15 mmol) was supplemented into the flask. The reaction was quenched 30 min later by the addition of H_2O (5 mL). CH_2Cl_2 and $NaHCO_3$ (sat. aq.) were subsequently added, and the organic phase was washed three times with $NaHCO_3$. The combined aqueous layers were extracted with CH_2Cl_2 once, and the combined organic layers were dried over Na_2SO_4, filtered, and concentrated. The residue was purified by flush column chromatography (SiO_2, 7:3 hexane/ethyl acetate) to yield compound **6** (1.43 g, 87%) as an amorphous yellow solid: ^{1}H NMR (500 MHz, chloroform-*d*) δ 9.00 (s, 1H), 8.76 (s, 1H), 8.16 (s, 1H), 8.01 (d, *J* = 7.6 Hz, 2H), 7.76 (d, *J* = 7.4 Hz, 2H), 7.60 (d, *J* = 7.4 Hz, 1H), 7.53 (t, *J* = 7.5 Hz, 4H), 7.39 (s, 2H), 7.28 (s, 2H), 6.05 (s, 1H), 5.75 (s, 1H), 5.32 (s, 1H), 4.65 (d, *J* = 7.3 Hz, 1H), 4.41 (dd, *J* = 10.5, 7.0 Hz, 1H), 4.36 (d, *J* = 6.5 Hz, 1H), 4.20 (s, 1H), 4.07 (s, 3H), 1.23−0.99 (m, 28H).; ^{13}C NMR (126 MHz, chloroform-*d*) δ 164.6, 153.0, 149.9, 143.7, 142.6, 141.5, 134.0, 133.0, 129.1, 128.0, 127.2, 125.2, 123.7, 120.3, 88.8, 84.0, 77.5, 77.4, 77.2, 77.0, 70.5, 67.4, 62.9, 57.2, 47.3, 17.7, 17.6, 17.5, 17.4, 17.2, 13.4, 13.4, 13.1, 12.9.; HRMS (ESI Q-TOF) *m*/*z*: [M + Na]$^+$ calcd for $C_{44}H_{54}N_6O_7Si_2Na$ 857.3465; found 857.3485.

*N^6-Benzoyl-2′-deoxy-2′-[(9-fluorenylmethyloxycarbonyl)amino]-adenosine (**7**).* Compound **6** (1.43 g, 1.71 mmol) was dissolved in THF (7.2 mL), and the reaction was stirred at ambient temperature under argon. TEA·3HF (0.48 mg, 0.91 mmol) was then added into the flask. The reaction was stirred for 10 h and subsequently quenched by the addition of excess methoxytrimethylsilyl. After 2 h, the reaction mixture was concentrated, and the residue was purified by flush column chromatography (SiO_2, 3% to 5% methanol in CH_2Cl_2) to yield compound **7** (0.74 g, 73%) as an amorphous solid: ^{1}H NMR (500 MHz, DMSO-d_6) δ 11.24 (s, 1H), 8.76 (s, 1H), 8.68 (s, 1H), 8.06 (d, *J* = 7.7 Hz, 2H), 7.85 (d, *J* = 7.6 Hz, 2H), 7.70−7.59 (m, 3H), 7.55 (t, *J* = 7.4 Hz, 3H), 7.38 (t, *J* = 7.4 Hz, 2H), 7.25 (dt, *J* = 30.3, 7.5 Hz, 2H), 6.18 (d, *J* = 8.4 Hz, 1H), 5.78 (d, *J* = 4.4 Hz, 1H), 5.24 (t, *J* = 5.6 Hz, 1H), 5.10−4.91 (m, 1H), 4.30 (s, 1H), 4.28−4.19 (m, 1H), 4.18−4.06 (m, 3H), 3.77−3.57 (m, 2H), 3.36 (s, 1H).; ^{13}C NMR (126 MHz, DMSO-d_6) δ 165.6, 155.9, 152.4, 151.7, 150.5, 143.7, 143.3, 140.7, 133.4, 132.5, 128.5, 128.5, 127.6, 127.0, 125.9, 125.4, 125.2, 120.1, 87.3, 85.7, 70.2, 65.9, 61.7, 56.8, 48.6, 46.5, 40.0, 39.9, 39.8, 39.7, 39.6, 39.5, 39.4, 39.2, 39.0, 38.9.; HRMS (ESI Q-TOF) *m*/*z*: [M + H]$^+$ calcd for $C_{32}H_{29}N_6O_6$ 593.2143; found 593.2128.

*N^6-Benzoyl-2′-deoxy-5′-O-[4,4′-dimethoxytrityl]-2′-[(9-fluorenylmethyloxycarbonyl)amino]adenosine (**8**).* Compound 7 (170 mg, 0.29 mmol) was co-evaporated with dried pyridine three times, then dissolved in dried pyridine (2.9 mL), and the mixture was stirred at ambient temperature under argon. 4,4′-*O*,*O*-dimethoxytrytyl chloride (117 mg, 0.34 mmol) was then added into the reaction mixture, and this was stirred for 4 h and quenched through the addition of excess methanol (2 mL). Next, CH_2Cl_2 and $NaHCO_3$ (sat. aq.) were added, and the organic phase was washed three times with $NaHCO_3$. The combined aqueous layers were extracted with CH_2Cl_2 once. The combined organic layers were dried over Na_2SO_4, filtered, and concentrated. The residue was purified by flush column chromatography (SiO_2, 8:2, ethyl acetate/hexane) to yield compound **8** (185 mg, 72%) as an amorphous solid: ^{1}H NMR (500 MHz, chloroform-*d*) δ 9.20 (s, 1H), 8.71 (s, 1H), 8.37 (s, 1H), 7.94 (d, *J* = 7.6 Hz, 2H), 7.67−7.51 (m, 3H), 7.49−7.37 (m, 6H), 7.31 (d, *J* = 8.5 Hz, 5H), 7.28−7.22 (m, 3H), 7.19 (d, *J* = 7.2 Hz, 1H), 7.14−7.07 (m, 2H), 6.78 (d, *J* = 8.2 Hz, 4H), 6.48 (d, *J* = 8.0 Hz, 1H), 6.31 (d, *J* = 7.9 Hz, 1H), 5.10 (d, *J* = 6.9 Hz, 1H), 4.67 (s, 1H), 4.48 (s, 1H), 4.33 (s, 1H), 4.29−4.18 (m, 1H), 3.98 (s, 1H), 3.73 (s, 6H), 3.51−3.31 (m, 2H), 2.38 (s, 1H).; ^{13}C NMR (126 MHz, chloroform-*d*) δ 165.1, 158.8, 156.6, 152.8, 152.4, 149.5, 144.6, 143.9, 143.8, 142.2, 141.4, 141.3, 135.8, 135.7, 133.7, 133.1, 130.3, 129.1, 128.4, 128.2, 128.1, 127.9, 127.8, 127.2, 127.2, 125.1, 125.1, 123.2, 120.1, 120.1, 113.5, 87.0, 86.5, 85.8, 77.6, 77.5, 77.3, 77.0, 72.0, 67.1, 64.0, 58.1, 55.4, 47.2.; HRMS (ESI Q-TOF) *m*/*z*: [M + Na]$^+$ calcd for $C_{53}H_{46}N_6O_8Na$ 917.3269; found 917.3282.

*N^6-Benzoyl-2′-deoxy-5′-O-[4,4′-dimethoxytrityl]-2′-[(9-fluorenylmethyloxycarbonyl)amino]adenosine 3′-(2-cyanoethyl N,N-diisopropylphosphoramidite) (**9**).* Compound **8** (520 mg, 0.58 mmol) was co-evaporated first with dried pyridine, followed by toluene and finally CH_2Cl_2. This was done 3 times with each solvent. Next, the dried compound was dissolved in anhydrous CH_2Cl_2 (5.8 mL), and the reaction was stirred at ambient temperature under argon. *N*,*N*-diisopropylethylamine (222 μL, 2.33 mmol) was added, followed by 2-cyanoethyl *N*,*N*-diisopropylchlorophosphoramidite (259 μL, 1.16 mmol), and this was stirred at ambient temperature over 1.5 h. Next, CH_2Cl_2 and $NaHCO_3$ (sat. aq.) were added, and the organic phase was washed three times with $NaHCO_3$. The combined aqueous layers were extracted with CH_2Cl_2 once. The combined organic layers were dried over Na_2SO_4, filtered, and concentrated. The residue was purified by flash column chromatography (SiO_2, 5:5 to 3:7, ethyl acetate/hexane) to yield compound **9** (500 mg, 79%) as an amorphous solid: ^{1}H NMR (500 MHz, chloroform-*d*) δ 9.12 (s, 1H), 8.77 (d, *J* = 9.3 Hz, 1H), 8.33 (d, *J* = 26.3 Hz, 1H), 8.02 (d, *J* = 7.6 Hz, 2H), 7.74 (t, *J* = 7.2 Hz, 2H), 7.59 (t, *J* = 7.4 Hz, 1H), 7.51 (t, *J* = 7.7 Hz, 4H), 7.47−7.40 (m, 2H), 7.41−7.17 (m, 11H), 6.81 (d, *J* = 8.6, 2.9 Hz, 4H), 6.26−6.02 (m, 1H), 5.87−5.48 (m, 1H), 5.31−5.03 (m, 1H), 4.77−4.54 (m, 1H), 4.53−4.20 (m, 3H), 4.18−4.05 (m, 1H), 3.91−3.56 (m, 7H), 3.57−3.42 (m, 1H), 3.36 (dd, *J* = 10.6, 3.6 Hz, 1H), 2.46 (dd, *J* = 5.9 Hz, 1H), 2.32 (t, *J* = 6.4 Hz, 1H), 2.02−1.84 (m, 1H), 1.35−1.02 (m, 14H).; ^{13}C NMR (126 MHz, chloroform-*d*) δ 164.6, 158.7, 156.0, 153.0, 152.9, 152.4, 149.6, 149.6, 144.4, 143.7, 141.8, 141.7, 141.4, 135.5, 133.9, 132.8, 130.2, 130.2, 130.2, 129.0, 128.3, 128.2, 128.1, 127.9, 127.8, 127.2, 125.1, 125.0, 124.9, 124.8, 123.2, 120.1, 117.5, 117.4, 113.4, 87.0, 86.5, 85.1, 77.4, 77.4, 77.2, 77.1, 76.9, 67.3, 66.6, 63.4, 58.7, 58.5, 56.9, 56.6, 55.4, 55.4, 47.3, 47.1, 43.7, 43.6, 43.5, 24.9, 24.7, 24.7, 24.6, 20.4, 20.0.; ^{31}P NMR (202 MHz, chloroform-*d*) δ 152.9, 151.7.; HRMS (ESI Q-TOF) *m*/*z*: [M + Na]$^+$ calcd for $C_{62}H_{63}N_8O_9PNa$ 1117.4348; found 1117.4331.

■ ASSOCIATED CONTENT

Supporting Information

The Supporting Information is available free of charge on the ACS Publications website at DOI: 10.1021/acs.joc.5b01719.

Additional data such as HPLC analysis, PAGE gels and ^{1}H, ^{13}C, ^{31}P NMR spectra (PDF)

■ AUTHOR INFORMATION

Corresponding Author

*masad.damha@mcgill.ca

Notes

The authors declare no competing financial interest.

■ ACKNOWLEDGMENTS

This work was supported in part by grants from the National Science and Engineering Research Council (to M.J.D.), Department of Veterans Affairs (1 I01 BX002580, to P.J.H.), the Robert A. Welch Foundation (AQ-1399, to P.J.H.), the National Science Foundation (DBI-0905865, to E.J.M.) the Judith and Jean Pape Adams Charitable Foundation (to P.J.H.), the Barshop Institute for Longevity and Aging Studies (5 T32 AG021890, to E.J.M. and N.E.C.), and a Strategic Young Researcher Overseas Visits Program for Accelerating Brain Circulation from a Japan Society for the Promotion of Science (JSPS).

DOI: 10.1021/acs.joc.5b01719
J. Org. Chem. 2015, 80, 10108−10118

REFERENCES

(1) Sharp, P. A. *Cell* **1981**, *23*, 643.
(2) Ruskin, B.; Green, M. R. *Science* **1985**, *229*, 135.
(3) Matera, A. G.; Wang, Z. *Nat. Rev. Mol. Cell Biol.* **2014**, *15*, 108.
(4) Will, C. L.; Lührmann, R. *Cold Spring Harbor Perspect. Biol.* **2011**, *3*, a003707.
(5) Brody, E.; Abelson, J. *Science* **1985**, *228*, 963.
(6) Murphy, W. J.; Watkins, K. P.; Agabian, N. *Cell* **1986**, *47*, 517.
(7) Chapman, K. B.; Boeke, J. D. *Cell* **1991**, *65*, 483.
(8) Nam, K.; Hudson, R. H.; Chapman, K. B.; Ganeshan, K.; Damha, M. J.; Boeke, J. D. *J. Biol. Chem.* **1994**, *269*, 20613.
(9) Ooi, S. L.; Samarsky, D. A.; Fournier, M. J.; Boeke, J. D. *RNA* **1998**, *4*, 1096.
(10) Okamura, K.; Hagen, J. W.; Duan, H.; Tyler, D. M.; Lai, E. C. *Cell* **2007**, *130*, 89.
(11) Ruby, J. G.; Jan, C. H.; Bartel, D. P. *Nature* **2007**, *448*, 83.
(12) Hasselberth, J. R. *WIREs RNA* **2013**, *4*, 677.
(13) Montemayer, E. J.; Katolik, A.; Taylor, A. B.; Scheurmann, J.; Combs, D. J.; Johnsson, R.; Holloway, S. P.; Stevens, S. W.; Damha, M. J.; Hart, P. J. *Nucleic Acids Res.* **2014**, *42*, 10845.
(14) Matange, N.; Podobnik, M.; Visweswariah, S. S. *Biochem. J.* **2015**, *467*, 201.
(15) Neumann, M.; Sampathu, D. M.; Kwong, L. K.; Truax, A. C.; Micsenyi, M. C.; Chou, T. T.; Bruce, J.; Schuck, T.; Grossman, M.; Clark, C. M.; McCluskey, L. F.; Miller, B. L.; Masliah, E.; Mackenzie, I. R.; Feldman, H.; Feiden, W.; Kretzschmar, H. A.; Trojanowski, J. Q.; Lee, V. M. *Science* **2006**, *314*, 130.
(16) Kwong, L. K.; Neumann, M.; Sampathu, D. M.; Lee, V. M.; Trojanowski, J. Q. *Acta Neuropathol.* **2007**, *114*, 63.
(17) Armakola, M.; Higgins, M. J.; Figley, M. D.; Barmada, S. J.; Scarborough, E. A.; Diaz, Z.; Fang, X.; Shorter, J.; Krogan, N. J.; Finkbeiner, S.; Farese, R. V., Jr.; Gitler, A. D. *Nat. Genet.* **2012**, *44*, 1302.
(18) Guschlbauer, W.; Krzysytof, J. *Nucleic Acids Res.* **1980**, *8*, 1421.
(19) Lackey, J. G.; Mitra, D.; Somoza, M. M.; Cerrina, F.; Damha, M. J. *J. Am. Chem. Soc.* **2009**, *131*, 8496.
(20) Katolik, A.; Johnsson, R.; Montemayor, E.; Lackey, J. G.; Hart, J. P.; Damha, M. J. *J. Org. Chem.* **2014**, *79*, 963.
(21) Matray, T. J.; Gryaznov, S. M. *Nucleic Acids Res.* **1999**, *27*, 3976.
(22) Lietard, J.; Ittig, D.; Leumann, C. J. *Bioorg. Med. Chem.* **2011**, *19*, 5869.
(23) Mignet, N.; Gryaznov, S. M. *Nucleic Acids Res.* **1998**, *26*, 431.
(24) Robins, M. J.; Hawrelak, S. D.; Hernandez, A. E.; Wnuk, S. F. *Nucleosides Nucleotides* **1992**, *11*, 821.
(25) Op de Beeck, M.; Madder, A. *J. Am. Chem. Soc.* **2011**, *133*, 796.
(26) Lohrmann, R.; Orgel, L. E. *J. Mol. Evol.* **1976**, *7*, 253.
(27) Krantz, A. *Bioorg. Med. Chem. Lett.* **1992**, *2*, 1327.
(28) Wang, H.; Hill, K.; Perry, S. E. *J. Biol. Chem.* **2004**, *279*, 1468.

DOI: 10.1021/acs.joc.5b01719
J. Org. Chem. 2015, 80, 10108−10118